Natural Hazards (2020) 103:3101–3121
https://doi.org/10.1007/s11069-020-04121-6

ORIGINAL PAPER

Mitigating drought and landslide simultaneously for mountain tribes of Taiwan: hydrogeological investigation, modelling, and development of an intelligent hazard prevention system

Hung-Chieh Lo[1] · Shih-Meng Hsu[2] · Po-Yi Chou[1] · Chien-Chung Ke[1]

Received: 6 March 2019 / Accepted: 16 June 2020 / Published online: 24 June 2020

Abstract

Drought and landslide are two common hazards that occurred in mountainous regions of Taiwan. This study is intended to develop a new concept of hazard prevention and management for solving both hazards simultaneously, in which the complex hazard has increased over the years in intensity and frequency due to climate variability and change. The proposed concept is a win–win solution that contains the feature of efficiency to mitigate two hazards together. When pumping groundwater as daily water demand at landslide-prone sites, the pore-water pressure decreases and the thickness of the unsaturated zone increases, which can result in stabilizing landslide-prone slopes and increasing flood storage capacity as an underground detention basin, respectively. Consequently, this approach can reduce the risk induced by the two hazards. To reinforce the effectiveness and instantaneity of hazard management, the technologies of smart sensing, smart transmission, and smart computing are then incorporated into a novel framework to develop an *intelligent hazard prevention and management system*. Thus, the groundwater supply-slope stability management system was installed and tested in the remote Kaoshi tribe, which is situated in Kaoshi Village of Mudan Township, Pingtung County, southern Taiwan. Hydrogeological issues for subsurface complexity, field investigations, and numerical modelling for preliminary evaluation and system design are also highlighted in this study. The developed system, which can offer valuable support for decision-making processes of hazard prevention, is capable of monitoring dynamic signals from various in-situ sensors, helping water resource allocations, and stabilizing hill slopes by means of drainage.

Keywords Intelligent hazard prevention and management system · Drought · Mitigation · Groundwater exploitation · Landslide · Internet of things (IoT)

✉ Shih-Meng Hsu
shihmeng@mail.ntou.edu.tw

[1] Geotechnical Engineering Research Center, Sinotech Engineering Consultant, 3F, No. 280, Xinhu 2nd Rd., Neihu Dist., Taipei City 11494, Taiwan, ROC

[2] Department of Harbor and River Engineering, National Taiwan Ocean University, No.2, Beining Rd., Zhongzheng Dist., Keelung City 20224, Taiwan, ROC

1 Introduction

Climate change has been a significant environmental concern affecting human lives over the decades. The following hazards, such as extreme rainfall events or prolonged dry periods, are increasing in intensity and frequency and vitally disrupt goals on global sustainable development (UNISDR 2015; World Bank 2015). Such influences also unavoidably occur in Taiwan and remain two significant impacts in mountainous regions: (1) imbalanced water resources availability, and (2) landslide hazards. For example, in the spring of 2015, Taiwan experienced its worst water shortage in 68 years. The severe water crisis dried out all reservoirs and significantly affected a million people's water use. In August of the same year, the typhoon Soudelor brought extreme rainfall to trigger the occurrence of large scale landslide in the upstream of Wu-Lai area. This devastating event not only blocked the road for people escaping to the safe place but also increased water turbidity in the downstream water treatment plant that restricted clean water supply a couple of days for residents in Taipei City. Such a hazard combined with drought and landslide has become a serious issue frequently affecting people's lives and causing property damages in the environment of mountain areas.

To deal with the complex hazard induced by drought and landslide, the traditional remediation remains on solving each type of hazard separately. Under the dilemma of the growing awareness of environmental protection against constructing a new reservoir, the primary countermeasures for mitigating drought are advocating joint operation, which is integrated multiple water resources and systems in the local region, and follow the policy of saving and producing recycled water simultaneously (Lai 2017). Most developed countries also make similar efforts in water saving, water use efficiency, and water recycling against drought (Estrela and Sancho 2016; Hong et al. 2016; Okada 2016). Concerning remediation of a destroyed slope, the conventional slope stabilization is to design the most cost-effective works for mitigating the sliding potential based on the failure mechanism and scale of landslides (Hutchinson 1984; Turner and Schuster 1996; SWCB 2014; Lin et al. 2018). One of the slope stabilization techniques is lowering groundwater to reduce pore water pressure in a stratum and subsequently increase effective stress (shear strength) through installing lateral drainage pipes or pumping wells. In general, the extracted groundwater is discharged to the surface drainage system with no further use. However, the extracted groundwater can be reused in a novel way. For example, the groundwater gallery built in the Li-Shang landslide area of Taiwan in helping slope stabilization constantly discharges over a million cubic meters of groundwater each year (SWCB 2011). If the drained water can be reutilized at proper management, the amount of groundwater can supply approximately 10,537 people for their daily water use. The alternative may become one of the solutions for conquering water shortages. From the perspective of water conservation, recycling the drained groundwater as an alternative water resource resembles fulfilling the concept of a circular economy.

While facing a complex hazard such as drought and landslide together, a novel concept to solve this type of problem is to adopt a total solution that contains the feature of efficiency to mitigate two hazards simultaneously. To achieve the goal, the solution for solving drought must get rid of pursuing the most exploited water (e.g. construction of a new reservoir). Instead of the traditional exploited way, 'harvesting' groundwater in an undeveloped mountain area only in accordance with local water demand is considered to be a better option. The hidden water resources can help the existing water resources allocation system withstand seasonal or erratic drought. Notably, this kind of water resources takes great advantage of water supply for specific occasions when the water supply is under an urgent situation. In the process of groundwater exploitation (dewatering), the drawdown of groundwater in the formation not only decreases pore water pressure but also produces more capacity to store extremely infiltrated rainwater in the formation, which is acting as an underground detention basin. The above two benefits result in improving slope stability and increasing flood storage capacity, respectively. Consequently, the risk of rainfall-induced slope and hazards is significantly reduced.

In addition to the concept of a total solution, timely and effective approaches are a vital element of hazard management for mitigation risks caused by natural hazards (Hany Abulnour 2014; Chen et al. 2016; Pal et al. 2017). With the aid of smart technologies [e.g. the Internet of Things (IoT)], hazard management can be accomplished in an easy way. In fact, IoT is an emerging technology devoted in numerous industries (Fang et al. 2013; Xi et al. 2018; Xu et al. 2018) and has been applied for water management (Verma et al. 2015; Geetha and Gouthami 2017; Narendran et al. 2017; Moulat et al. 2018) and landslide monitoring (Wang et al. 2013; Yang et al. 2017). However, such applications are rarely used for simultaneously mitigating drought and landslide.

Based on the problem and concept mentioned above, this study proposes an *intelligent hazard prevention and management system* to mitigate drought and landslide simultaneously for mountain tribes of Taiwan. Hydrogeological investigations, modelling and development of the intelligent system were conducted and demonstrated in a selected mountain indigenous village of Taiwan with the historical record of landslide and drought. At first, the hydrogeological investigations in the study site were to clarify complicated hydrogeological properties and to obtain various parameters for a proposed numerical model. Secondly, the hydrogeological conceptual model, combined with the investigated data, was established to simulate various hazard prevention and management scenarios. Thirdly, the intelligent system, including monitoring devices (piezometer, flowmeter, pump, pumping controller, data logger, etc.), solar energy, and IoT technology, was installed on the site. Due to the installation of solar panels and batteries, the system owns an energy independent solution. After completing the installation of all hardware, the real-time data, including changes in the water level, pumping rate, and power consumption, can be remotely transmitted to the database, and allow users to track the effectiveness of groundwater exploitation and daily water usage. By the aid of numerical simulation results, the slope stability of the study site can be monitored through water level data as well. In addition to the function of monitoring data, users can remotely activate the water pump not only for their water demands but also for reducing landslide hazards. Such an application of IoT remains a significant advantage via self-controlling the system and adjusting the groundwater level while facing urgent situations associated with landslide and drought.

2 Description of the study area

The study area is situated in Kaoshi Village of Mudan Township, Pingtung County, southern Taiwan, as shown in Fig. 1. Kaoshi Village, which has a population total of 711 and an area of 25.54 sq. km, is an indigenous mountain village. The main population in the village is the Paiwan people of the Taiwanese aborigines. The Kaoshi village is geographically divided into three subtribes (upper, middle, and lower). The lower tribe is close to the Zhonggang creek that passes through the village from north to south and flows into the sea.

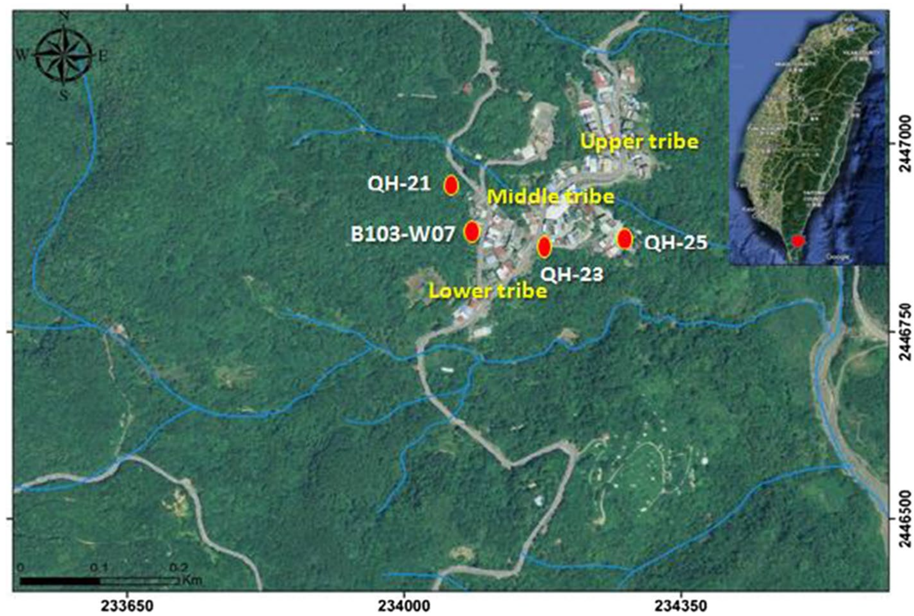

Fig. 1 Locations of the study area and investigated boreholes

Historical rainfall data (2006–2010) collected from a neighbouring rain gauge station showed the annual precipitation was 3479 mm, mainly accounted for 76.3% from May to September. The highest amount was 642.5 mm in July, while the lowest was around 77.6 mm in January (WRA 2011). The annual accumulated rainfall of this area was more than the average annual rainfall of Taiwan, which is about 2500 mm. Due to the exceptional rainfall, the area is vulnerable to hydro-geo hazards. Typhoon Morakot in August 2009 induced a severe landslide event that struck the area and destroyed houses, retaining walls, and the roads. The water supply system of this area was also slammed, led to water shortages and restrictions. After the landslide hazard, some residents were relocated to the temporary sanctuary until their houses were rebuilt, and the Kaoshi village was officially identified as a landslide-prone area (Hsu et al. 2012). Various signs of landslides, such as tension cracks in the pavement and retaining wall, house subsidence, and leaning electricity poles, can currently be seen in the tribe. These signs indicate the area is undoubtedly prone to landslides.

As for the regional geology of the Kaoshi village, the village is dominated by the Mudan formation of late Miocene, which mainly consists of shale interbedded with thin sandstone. Slump structures are frequently found. These observations reveal that the formation is displaced or moved due to the steep slope or fast sedimentation rate in the study area. This finding also shows possible evidence of ancient slumps.

In addition to the risk of landslides, the village is also facing unusual water scarcity that is lack of water resources to meet the local water demand during the specific period (typhoons and drought years). The reason is that the village has no tap water system that entirely relies on taking water out of an upstream river. When facing typhoon events, the source of water is easily be blocked by rainfall-induced local landslides or debris flows. While suffering from a drought year, the creek and ponds nearby the village are all dry;

apparently, an insufficient water resource in the tribe is obvious. Therefore, their water supply system is at risk from a sustainable point of view. In order to solve water shortage problems, some residents themselves installed wells directly, extracting the groundwater for their daily water demand. One of the wells was found in the field, which has 3.4 m in depth and supplies water for eight families. To sustain the mountain tribe's sustainable development, imbalanced water resources availability and landslide hazards have to be solved simultaneously.

3 Methodology

The purpose of this study is to develop an innovative system for effectively exploiting groundwater resources and simultaneously stabilizing slope at a landslide-prone site of the remote Kaoshi tribe. Since groundwater flow properties and geological characteristics in the subsurface of the study site are invisible, adequate characterization and modelling of the study site as well as constructing a smart monitoring and controlling system are crucial tasks for optimizing the system; namely, customizing the capacity in accordance with site conditions and maximizing system efficiency with minimal cost. The three steps of developing the intelligent hazard mitigation system include: (1) performing hydrogeological investigations (borehole drillings and hydrogeological tests) in a selected active landside site, (2) constructing a hydrogeological conceptual model based on the investigated outcome of the first stage and performing numerical studies to understand groundwater flow and slope stability of the study site, and (3) design and establishment of the intelligent hazard prevention system.

3.1 Site investigation

In light of a preliminary field survey on the potential of landslide and resident inquiries for the drought impact issue, this study selects the lower tribe of Kaoshi Village as a major investigated area. The study area is located between Mountain Kaoshi and River Zhonggang, with an area of 50 acres. The elevation of the study area ranges from 100 to 370 m above sea level. The average slope angle of the terrain equals 18.5° and descends from the west towards the east. The first step in developing the intelligent system is to understand the hydrogeological conditions of the site, which is a preliminary step for conducting numerical modelling. Four geological boreholes along the slope, as shown in Fig. 1, were drilled into the subsurface at depths ranging from 50 to 95 m at the test site for collecting rock core sample data. The rock core data were utilized for constructing a geologic cross section along the slope. Subsequently, a series of borehole exploration techniques, including televiewer logging, caliper logging, electrical logging, sonic logging, heat-pulse flowmeter logging, and packer test, were performed. The borehole exploration is an in-situ measurement that directly acquires a variety of subsurface hydrogeological characteristics, such as the distribution of lithology and fracturing and aquifer's hydraulic properties (Ku et al. 2009; Chou et al. 2012, 2014). All logging results were integrated using the WellCAD software for interpretations on not only clarifying the complexity of subsurface conditions but also delineating aquifer's potential water-bearing zones. Besides, the pumping test was conducted for targeting at a water-bearing zone, where the hydraulic parameters were obtained, and the groundwater availability for village residents can be assessed. After completing all hydrogeological tests, pressure transducers installed in the drilling boreholes to monitor groundwater level data as inputs for the model's calibration and simulation.

3.2 Numerical modelling

To produce groundwater that serves as the source of back-up water and to simultaneously reduce trends of rising groundwater level that improves slope stability, the authors established an appropriate numerical model that provides a crucial guideline to understand the groundwater flow and slope stability of the study area. The model is capable of computing the factor of safety (FOS) of the slip surface under various scenarios of groundwater exploitation and even determining the relationship between the amount of groundwater production and improvement in slope stability.

The conventional slope stability analysis for engineering practice is generally to input the groundwater level as the hydraulic condition in the model, rarely considers the rainfall infiltration process in unsaturated zones, which may significantly influence the variation of groundwater level with time. To improve the accuracy of simulated outcome which met reality, the study adopted a 2D time-dependent infiltration-seepage-stability coupled hydrogeological model known as Geostudio to simulate groundwater flow and slope stability for the Kaoshi landslide site (GEO-SLOPE International Ltd. 2007a,b). The finite element seepage module SEEP/W was used for the analysis of groundwater flow. The daily rainfall was applied as the boundary condition in the model, and the time-dependent seepage behaviour in a saturated–unsaturated medium was simulated. The coupled seepage-stability analysis was carried using a limit equilibrium analysis module SLOPE/W, which was able to compute the FOS of the slip surface under different distributions of water pressure induced by rainfall infiltration, evaporation, and groundwater discharge.

Since the model is a simplified representation of a complex hydrogeological condition, in order to improve the rationality, the calibration and verification of model parameters and boundary conditions are crucial tasks (Lo et al. 2010). For seepage analysis, the hydraulic properties of each geological unit were given by the results of the field packer test, and the daily rainfall data were set as the boundary condition on the top of the slope surface. The observed piezometric data were used to calibrate the hydraulic parameters and boundary conditions, namely, minimize the water level divergences between the numerical simulation and observed data. Subsequently, the calibrated model was verified by pumping test data. For stability analysis, the mechanical properties applied in the model were based on laboratory tests, such as physical properties test, direct shear test, and triaxial test. The results of coring and borehole logging data were used to delineate the potential slip surface. The integrated seepage-stability analysis was carried out to compute the dynamic change of a FOS induced by groundwater level fluctuations.

In order to plan the specific hazard protection strategies and prevention actions, the verified numerical model was used to realize the reaction of the landslide aquifer at all possible hydraulic scenarios. The results were considered to be the decision-making guideline for hazard management and the design of an intelligent prevention platform. According to the operation demand of the platform, for realizing the relationship between the groundwater harvesting and slope stability of the Kaoshi village, the study performed seepage-stability analysis and computed the FOS of the slopeland in response to the groundwater level under different pumping rates. The relationship provided substantial evidence in assessing the ability to exploit the groundwater for village people and mitigate the landslide risks. The process of modelling is shown in Fig. 2.

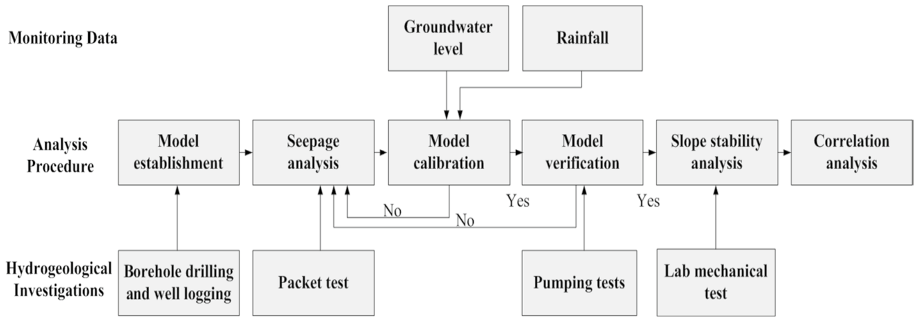

Fig. 2 The process of numerical modelling

3.3 Establishment of the intelligent system

The study developed an innovative, intelligent hazard prevention platform to help meet the trend of hazard prevention and management. By the aid of information communication technology, the system integrated smart sensors, smart communication, cloud computation, and solar panel technology to monitor the real-time groundwater fluctuations and immediately to pump out the water, which not only provided the sustainable water resources for tribal residents but also attained landslide hazard prevention and mitigation.

The components of the system listed in Table 1 consist of a 320 W solar panel, solar panel controller, 1HP submersible pump, power converter, flowmeter, piezometer, solid-state relay (SSR), signal amplifier, 4G communication module, electricity leakage breaker (ELB), data logger, and two 12 V/100AH batteries. In addition, a water tank was installed to store the pumped water for water allocation. The piezometers, allowed users to track the current water availability, were set inside the tank and pumping well. When water table data combined with the flowmeter data (recording how much water to be extracted), the integrated data were regarded as the basis for water resource allocation and hazard prevention management. The solar penal and battery were the source of electricity for the water pump, data logger, and data transmission module. The 4G communication module was set

Table 1 The system components and functions

Components	Functions
4G communication module	Transmit data to a server
Data logger	Store monitoring data
Piezometer	Monitor groundwater level
Flowmeter	Monitor pumping rate
Signal amplifier (AMP)	Amplify monitored signal
Submersible pump (1HP)	Extract water
DC-to-AC converter	Convert 24 V DC to 220 V AC
Solid-state relay(SSR)	Switch control pump on/off
Solar panel	Provide battery power
Solar panel controller	Protect battery overcharge
100AH/12 V battery	Store system power
Electricity leakage breaker (ELB)	Protect electric circuit overload

for instantaneous data transmission, including water level, flow rate, and battery power. The auto-control system was applied and able to activate the pump when the water level was at an urgent situation (e.g. groundwater rises above the warning level of landslide or water in the tank near empty). The functions of all components are also listed in Table 1. The configuration of the system is shown in Fig. 3. It can be seen that the solar panel charges the battery. The power is then transmitted to two paths: the first one is DC/AC converter that delivers the power to solid-state relay (SSR) and the pump; the second one is the power for the rest of the devices.

Since the capacity of the system power is highly related to aquifer conditions (i.e. water level, well yield, drawdown duration), it is essential to collect the groundwater monitoring, numerical modelling and pumping test data to design the system, such as the capacity of the pump, solar panel and battery, and location of piezometer and pump. The process is described below.

1. Collect long-term groundwater monitoring data to decide the depth of the pump and piezometer and maximum drawdown.
2. Predict the relationship between drawdown, pumping rate, and duration from pumping test to evaluate the battery capacity for pumping.
3. Determine the relationship between the drawdown and rising ratio in slope stability from numerical modelling to evaluate system efficiency for the groundwater yield and the increase in slope stability.

Finally, the Visual Basic.NET was adopted to construct a real-time platform that could monitor and control the in-situ system through the internet. The voltage of the battery was also recorded to track power consumption through the operation. In this platform, users could remotely send commands to activate the pump. At the same time, the groundwater level and outflow were recorded and displayed for real-time monitoring. In addition, the platform allowed users to set the upper and lower bound of water level so that the system could self-control the pump while the groundwater level reached the alarm value. This is the function that intelligently reduces the landslide potential for a heavy rainfall event. As for the operation of water supply, the system under a safe well yield automatically pumps

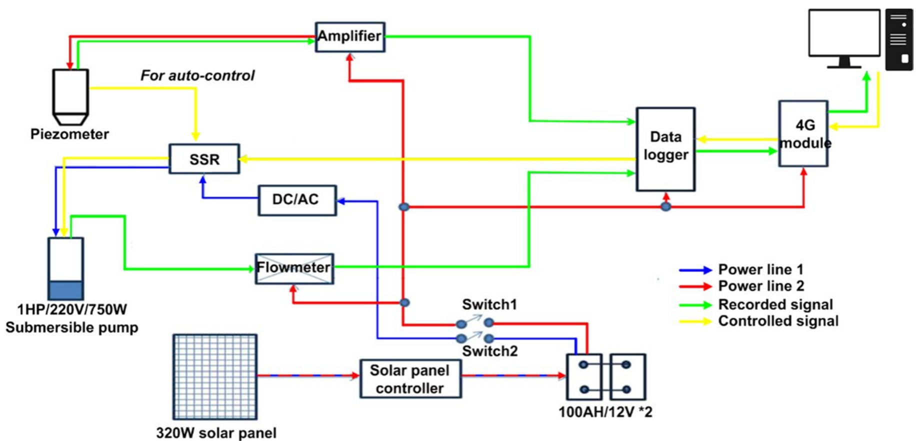

Fig. 3 System configuration

water as alternative water resources for tribal residents based on the water demand for both normal and urgent period. This is also the function that intelligently reduces the risk of drought-induced by climate change or damages of the water supply system.

4 Results and discussions

4.1 Hydrogeological conceptual model and model calibration of the landslide site

According to the results of four geological drilling boreholes, the lithostratigraphic classification for the geological cross-section of the slope was carried out. The strata can be divided into four layers from top to bottom: (1) The regolith layer was composed of about 6 m colluviums deposits; (2) The shear zone consisted of clayey shear materials and was usually considered to be a potential slip surface that may affect slope stability; (3) The fractured bedrock layer comprised shale or sandy shale, with very low RQD and several wide clayey shear bands; (4) The bedrock layer mainly consisted of shale or sandy shale, with small amount of shear bands. In addition to the obvious slip surface as shown in the second layer, other thick shear bands appeared in the fractured bedrock, and bedrock layers might continuously evolve to become potential slip surfaces if no further remediation of the slope was developed.

By means of various single borehole hydrogeologic tests in boreholes, the most important hydrogeologic features of the landslide site were explored. Figure 4 shows the investigation results carried out in borehole B103-W07. The televiewer and caliper (CALP) logging revealed the fracturing degree of the bedrock layer was intensive, and several clayey shear bands existed at the depths of 37–40 m, 42–54 m, 62–65 m, 67.5–70 m and 84–87.5 m, respectively. The flowmeter logging indicated the fractures at the specific depths (40 m, 78 m, 84 m, and 90 m) were connected to the hydraulic head that created a recharge/discharge flow into the borehole. This finding demonstrates that the geological heterogeneity of the site leads to a complicated groundwater flow system induced (Lo et al. 2014). Most of the locations with the signals of strong water exchange were found at the interface between the bedrock and shear band, which possibly indicate the continuous flow could be an impact to weaken the interface and to become a slip surface eventually. The results from two geophysical loggings (electrical logging and sonic logging) showed the values of both short and long normal resistivity (SHN and LON), single-point resistance (SPR), and sonic travel time were low, while those of gamma radiation (NGAM) were high. These low values from different signals with no apparent changes along the borehole imply the strata mainly consists of clayey material, such as shale, sandy shale, and shear bands. However, few places along the borehole show sharp deflections in single-point resistance and gamma radiation (i.e. 46–47.5 m, 55–57 m, 61 m and 70–72 m) due to the existence of thin layered sandstone. The explanation from various signals about the strata's lithologies also confirms the result from the borehole drilling.

The hydraulic parameter of a pack-off interval from the double packer test was analyzed using the software of AQTESOVE, which allowed both virtual and automatic curve matching (Duffield 2004). The results showed wide hydraulic characteristics in different geological layers. The hydraulic conductivity of colluvium ranged from 2.7×10^{-5} to 8.5×10^{-6} m/s, while the hydraulic conductivity of fractured bedrock and bedrock ranged from 5.4×10^{-6} to 1.3×10^{-8} m/s. The lowest hydraulic conductivity appeared in the bedrock layer, and its hydraulic conductivity was approximately 6.7×10^{-10} m/s. By integrating

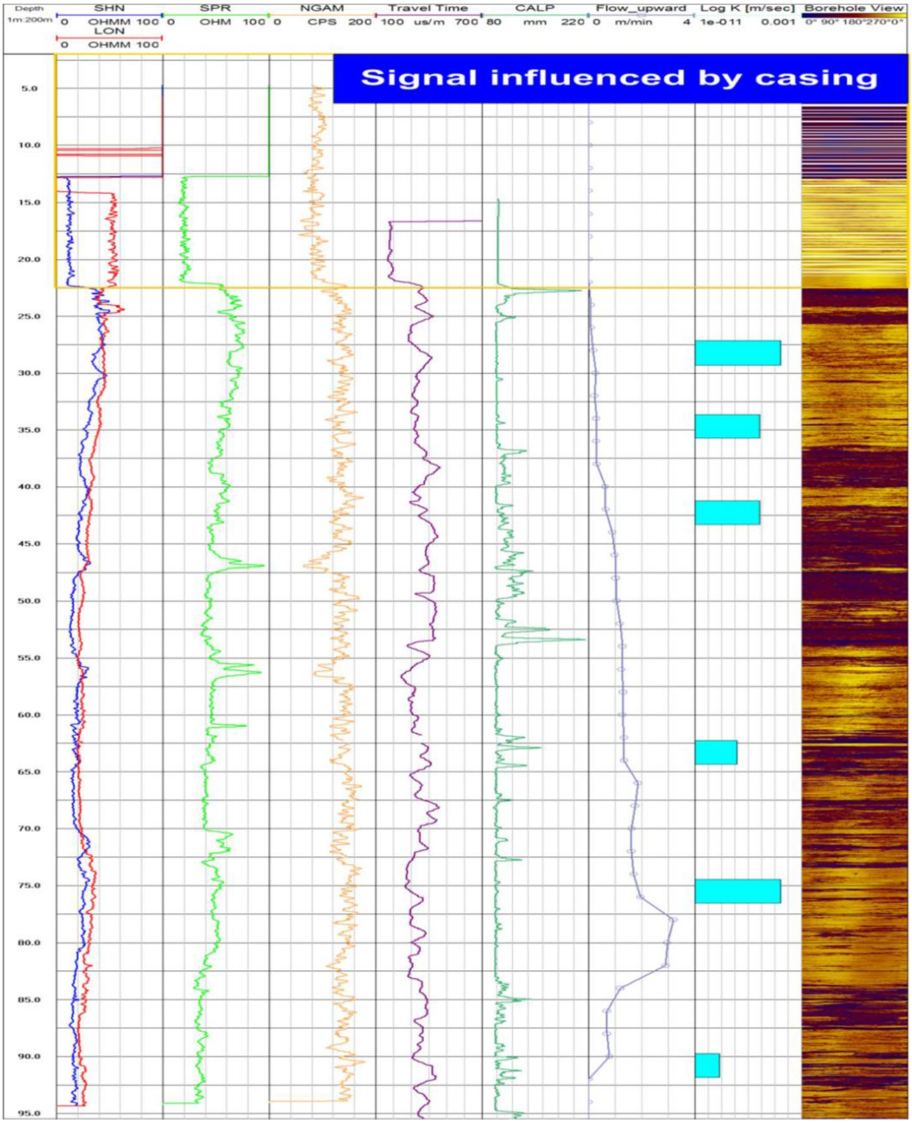

Fig. 4 Various down-hole investigation results conducted in borehole B103-W07

all hydraulic data, the water-bearing zone at the depth from 28 to 40 m was identified. This identification was used to design a pumping well for performing pumping tests and a monitoring well for collecting continuous groundwater level data.

Collections of the above abundant and diverse data from the direct in-situ investigations and measurements would facilitate the construction of the hydrogeological conceptual model of this landslide site. Therefore, this study integrated the aerial photography, borehole drilling data, and well logging data to build a hydrogeological conceptual model, as shown in Fig. 5. The strata of this study site are composed of four

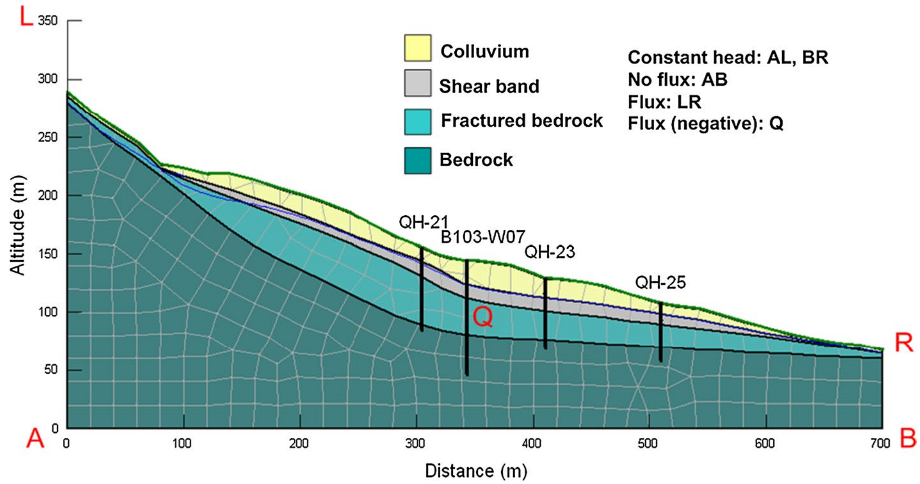

Fig. 5 The hydrogeological conceptual model of Kaoshi landslide site

layers (colluvium cover, shear zone, fractured bedrock, and bedrock) from top to bottom. The boundary conditions of the model are also shown in Fig. 5. Considering the strata is less permeable, and the change in groundwater level is not obvious, a constant head is given in specifying the upper and lower boundary condition. The fixed head is at the right and left side, while zero flux is at the bottom. The monitored rainfall data were applied as the recharge flux on the slope surface, and a negative flux is set in the same place of pumping test while simulating dewatering. The depth of slip surface was delineated at the interface between colluvium and shear band layer, which was based on the results of borehole drilling and well logging. The hydraulic conductivity used in the model was relied on the results of the packer test, while other parameters, including unit weight, water content, cohesion, and friction angle, were adopted from the results of the laboratory test. Finally, the model incorporating various mesh sizes has been tested. It turned out that the sensitivity of the mesh size to the modelling result was not noticeable. The fact was similar to Hoang et al. (2014), who found that the simulated water level varied less than 7.6 cm by changing the mesh size within the range of 15–25 m.

After completing the setup of the numerical model and the preparation of the parameters, the engineering software Geostudio was used for seepage and slope stability analysis. However, to provide a closer match to field situations for the developed model, the 5-months precipitation and groundwater monitoring data from June to November 2013, were used to calibrate the model's hydraulic parameters. Figure 6 illustrates the calibration result in terms of the transient groundwater levels between the observed and computed data with a similar trend. The average error between observed and simulated groundwater levels was 7.08% for borehole QH-21 and 3.54% for borehole QH-23. Finally, by applying the same pumping rate of 1.8 L/min for 12 h, the simulated yield per unit drawdown was 0.01 cmh/m. As compared to the result derived from the real pumping test (0.019 cmh/m), the present model was verified to be able to represent the real condition.

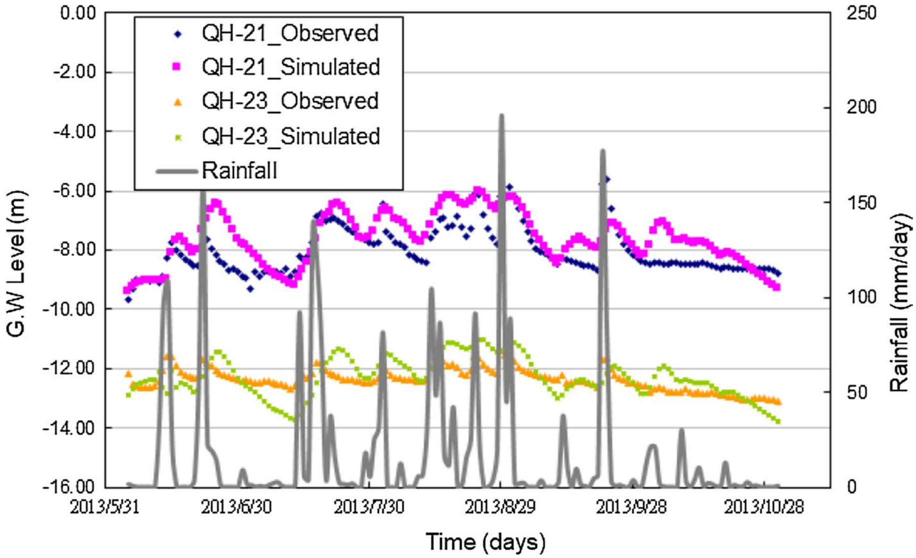

Fig. 6 The comparisons of simulated and observed groundwater level for boreholes QH-21 and QH-23

4.2 Groundwater availability and slope stability analysis

To understand the status of exploitation of groundwater resources, groundwater potential in the landslide site needs to be estimated. The constant rate pumping test was then conducted with the Moench (1997) solution to directly obtain the hydraulic parameter (transmissivity) as shown in Fig. 7 (blue circle: drawdown data; red line with the pumping rate of 1.8 L/min: type curve to the test data). A step-drawdown test evaluated the constant rate before the pumping test. In this study, the constant rate is regarded as the well yield of a borehole that is a reliable long-term yield (or safe yield) of a aquifer to ensure enough water that can be pumped out. As the results showed, the transmissivity and well yield of the test site were 2.876×10^{-5} m^2/min and 1.8 L/min, respectively. Two parameters are crucial information associated with in-situ groundwater availability for village residents.

Based on the estimated hydraulic parameter, a simple prediction can be taken for the possible extent of drawdown when different pumping rate is applied. Figure 7 illustrates various time-drawdown diagrams with varying rates of pumping. The prediction chart revealed that the higher the pumping rate, the shorter the pumping duration. However, such a case produces less water yield. For example, when the pumping rate is at 50 L/min, 8 m drawdown needs two minutes to reach and produces 100 L water yield. With the same amount of drawdown, when the pumping rate decreases to 10 L/min, the pumping duration extends to 50 min, and the water yield rises to 500 L.

In addition, with the calibrated numerical model as described in Sect. 4.1, the slope stability analysis was performed to investigate the status of slope stability at the landslide site. Figure 8 shows that the FOS of the slip surface in a period of rainy time ranges from 1.38 to 1.42, demonstrating that the landslide site tends to be stable after Typhoon Morakot. The simulated outcome is confirmed by the observed inclinometer measurement, which shows a slight change of the displacement about 0.78 cm through

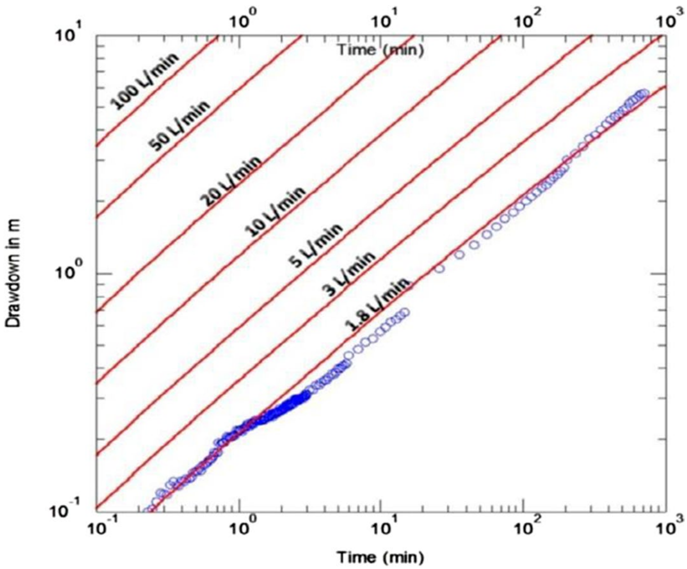

Fig. 7 Pumping test result and the predicted relationships among pumping rate, drawdown, and duration

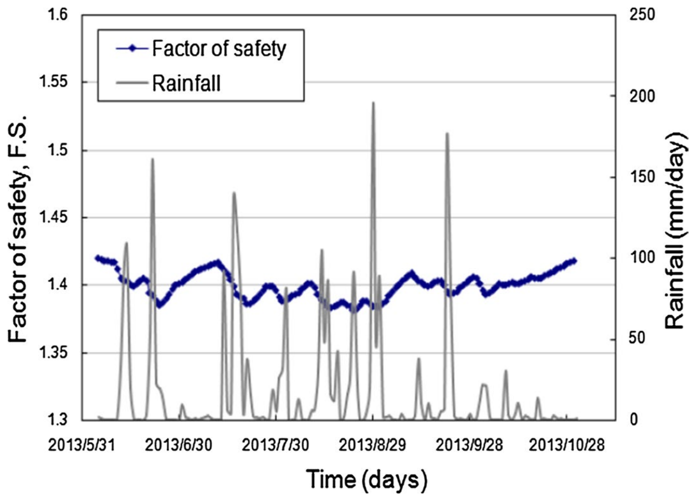

Fig. 8 Simulated results for modelling the FOS of slip surface during a rainy time

the monitoring period from June to November 2013, as shown in Fig. 9. The slight change of FOS also reveals the slope stability is not sensitive to the rainfall if it is less than 200 mm/day. However, the landslide risks still exist if the weathering and erosion processes of rock formation sustain or other extreme rainfall events occur. To diminish the landslide risks, the site needs a long-term monitoring and management system as well as performing appropriate stabilization methods against sliding potential.

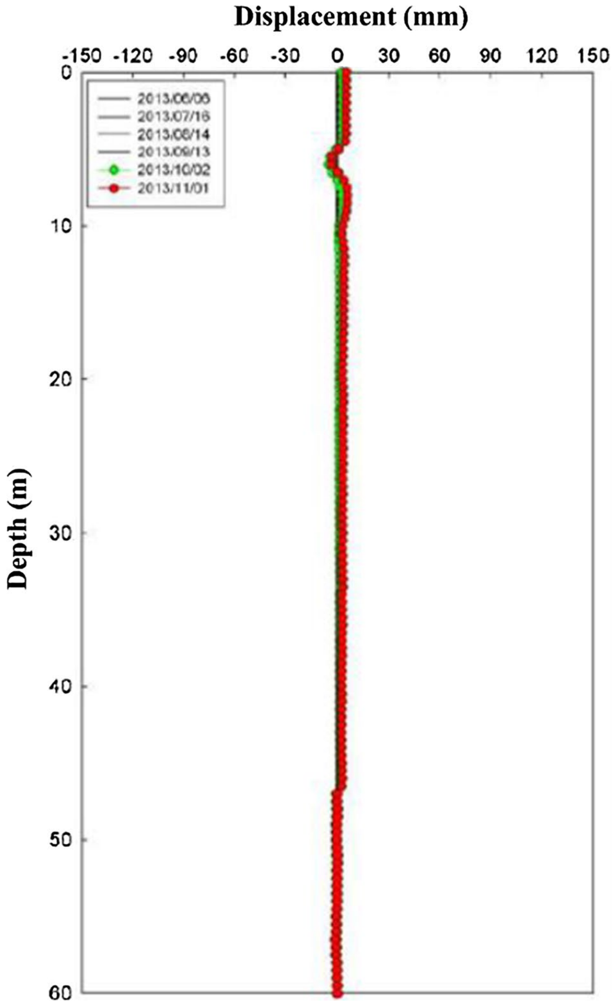

Fig. 9 The result of inclinometer measurement near the testing well

4.3 Scenarios simulation for drought and landslide risk management strategy

Once the model rationality has been validated, it is adopted to establish the relationship between pumping rate, pumping duration, and the change in FOS of the slip surface, which is considered to be the guideline for risk management of landslide and prevention of drought for the study area. At first, the study simulated the dewatering of the landslide site by applying the same pumping rate of 1.8 L/min for 12 h in borehole B103-W07. Figure 10 compares the change of groundwater level before pumping and after pumping. The result showed the groundwater level at the top of colluvium decreased to that at the bottom of colluvium. Accordingly, the value of FOS increased by approximately 10% as compared to the slope stability before pumping. The correlation analysis was then conducted to establish the relationship between pumping rate and FOS as well as the one between drawdown and FOS.

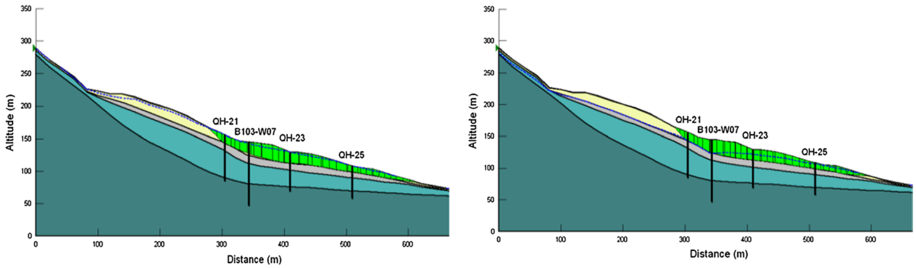

Fig. 10 Slope stability analysis for dewatering of Kaoshi landslide site: (Left) before pumping; (right) after pumping

Secondly, the study simulated variations of drawdown and rising ratio in FOS by applying 24-h pumping tests with various constant rates. Figure 11 shows two positive relationships between the pumping rate and the drawdown, as well as the pumping rate and the rising ratio in FOS. It demonstrated that the higher the pumping rate, the larger the drawdown and rising ratio in FOS. For example, when the pumping rate is set at 5 L/min for the pumping duration of 24 h, the water level declines to near the bottom of the fracture bedrock layer. The total drawdown is approximately 43.8 m, and the rising ratio in slope stability is about 23.7%. The above simulation results can directly establish the relationship between drawdown and slope stability. As a result shown in Fig. 12, a positive trend indicated the greater drawdown, the higher FOS.

Fig. 11 Relationship between pumping rate, drawdown and rising ratio in FOS

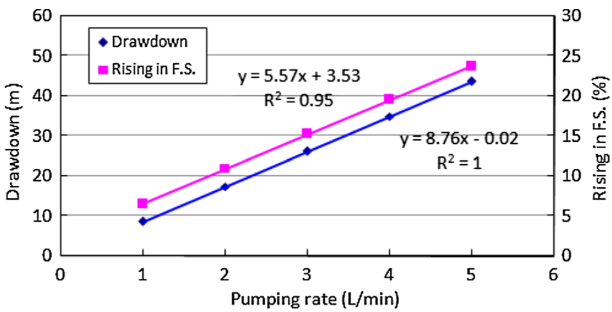

Fig. 12 Correlation between drawdown and rising ratio in FOS

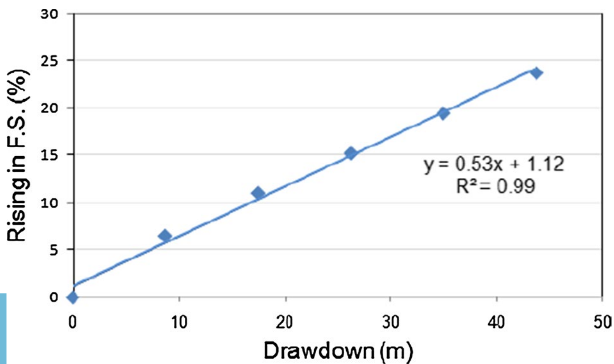

Finally, the study simulated variations of pumping duration and rising ratio in FOS by changing various constant rates under the condition of the maximal drawdown that the water level reached to the bottom of the fracture bedrock layer. Clearly, the results in Fig. 13 show both pumping duration and rising ratio in FOS have a negative trend with different pumping rates. The negative trend is due to the hydraulic property of the formation. Since the geologic formation at the study site is relatively impermeable, when the higher pumping rate is applied, the formation is unable to rapidly provide groundwater supply towards the well. Instantaneously, an induced quick drawdown in the well itself occurs due to the wellbore storage effect. In contrast, the formation is capable of providing a stable supply of groundwater under the lower pumping rate. For example, when the pumping rate is set at 2 L/min, the groundwater level needs 7.9 days to reach the maximal drawdown; approximately 22,752 L water is pumped out; this drainage effort for the slope stability increase about 29.1%. On the contrary, when the pumping rate rises to 5 L/min, the groundwater level in the well only needs one day to attain the same drawdown; due to the shorter pumping duration, only 7200 L water is pumped out; the corresponding rising ratio in slope stability is about 23%, which is less than the previous case. Thus, the rising ratio in slope stability depends on the amount of groundwater drainage; the more groundwater drains from the formation of the slope, the higher the FOS value produces. The pumping duration relies on a propagation speed of groundwater towards the well; the longer the pumping duration, the more stable the propagation speed of groundwater. A similar trend can also be found in Fig. 7, which shows that when the drawdown is fixed, the lower pumping rate requires the longer duration.

The simulation also reveals that although the drawdown is set at the same magnitude, the rising ratio in FOS under different pumping duration is slightly different. This deviation may be attributed to the fact that the radius of influence for longer pumping duration is wider than that for a shorter duration. The wider radius of influence may improve slope stability more. Overall, the above analysis produces practical pumping strategies on strengthening the slope stability and operating the supply of water resources to this community without aquifer overexploitation.

4.4 The intelligent management platform (installation, testing and platform)

According to the groundwater potential and local water demand of the Kaoshi village, the smart hazard prevention system was designed and installed in the field next to borehole B103-W07, as shown in Fig. 14. The present energy system has one 320 W solar panel and two 12 V/100AH batteries, which can supply the power continuously pumping water for

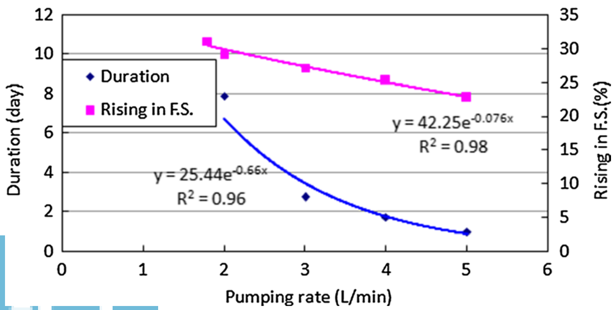

Fig. 13 Relationship between pumping rate, pumping duration and rising ratio in FOS

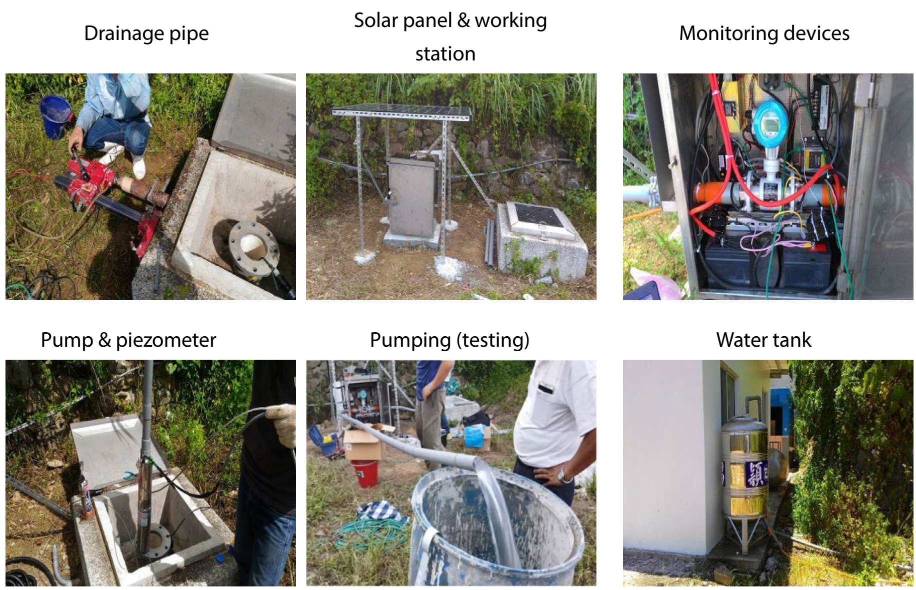

Fig. 14 Various components of the intelligent hazard prevention system installed and tested at the landslide site

2.65 h. The charging time for two batteries is 12.5 h to be fully charged. It is expected that the pumping system can operate one time on one cloudy day. The water yield and water demand for residents can be proposed and estimated in terms of the relationships between battery capacity, solar panel power, water pump power, and aquifer hydraulic properties.

Furthermore, due to the complexity of the subsurface hydrogeological condition, the drawdown, duration, and groundwater recovery from numerical modelling may remain some divergences to those observed from real testing. Figure 15 demonstrates one of the testing cases applied in the Kaoshi landslide site. For this test, a fixed pumping rate of 60 L/min, which is much higher than the safe yield of the aquifer (1.8 L/min), was performed to test how fast the groundwater would drop in a target depth (8.3 m) and how long the groundwater level for this aquifer system would come back to the original one after the pumping ceases. Results for this type of testing showed the groundwater level rapidly

Fig. 15 Drawdown obtained from real pumping in the Kaoshi landslide site

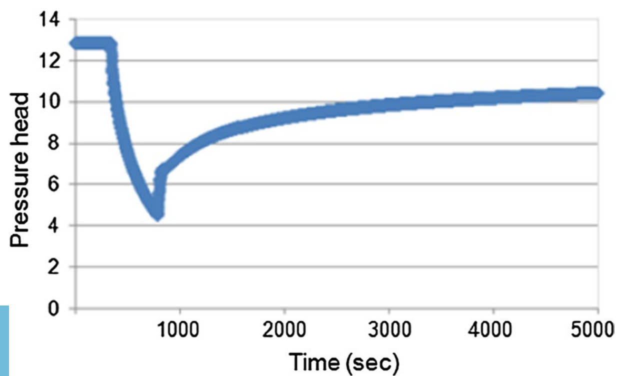

dropped 8.3 m in 448 s (7.5 min). The time spent was much longer than the simulated time, which was 1.7 min, as shown in Fig. 8. This testing result shows the groundwater productivity obtained from the field test has much more potential than that from the predicted outcome. This finding also confirms the complexity of subsurface hydrogeological conditions for predicting the performance of the aquifer employing a numerical model. Additionally, when shutting down the pump, the groundwater level takes 4210 s (70.1 min) to recover about 71% of the initial groundwater level. The quick dropping rate and long recovery rate of groundwater level indicate the groundwater potential at the site is not as good as alluvial aquifers, and the site is not suitable for long term dewatering. However, the groundwater potential from the current aquifer is sufficient to provide the residents of the Kaoshi tribe with urgent water resources. In the last analysis from this trial, this pumping operation produced a groundwater yield of 450 L, and the predicted slope stability increased around 7%. From experience on checking real groundwater productivity, the predicted rise in slope stability may be confirmed from real landslide deformation monitoring if available.

Finally, a web-based operating platform has been constructed, as shown in Fig. 16. For manual control, users can click "START" bottom to send the command to SSR via 4G module and then trigger the motor for pumping. At the same time, the piezometer records the change of water level and pressure head; flowmeter records flow rate, accumulated flow, and duration. The instantaneous data can be seen in the platform, as shown in Fig. 16a. All recorded data are saved in a data logger and sent back to the cloud system for a time series monitoring, as shown in Fig. 16b. In addition, the platform allows users to set the upper and lower bound of the groundwater level for automatic control. Once the water level reaches the upper threshold value, the SSR automatically starts the pump to lower the water level. Until the water level dropped to the lower bound value, the SSR shuts down the pump. This is the function to intelligently lower the groundwater level when it reached the warning level, which significantly reduces the landslide potential during heavy rainfall. Another application of the developed platform is regarded as a controller of water supply against the drought. Based on both constant and emergent water demand from the Kaoshi community, manual or automatic controls in the platform can also be set to withstand drought and potential landslides.

5 Conclusions

The concept of this study is originated from the idea of promoting life, safety, ecology, and sustainability of mountain tribes and relieving the impact associated with drought and landslide. A smart pumping system integrates solar energy, monitoring devices, a communication module, and a displayed platform, was successfully developed. After numerous trials in the Kaoshi landslide site, the system is confirmed useful to effectively exploit the groundwater and increase the slope stability. The conclusions are summarized as follows:

1. The system allows tribe residents remotely controlling the pump to satisfy their water demand and tracking the water usage, particularly when facing a period of drought.
2. The IoT helps the system automatically pump the water, benefit in improving early warning and response to landslide hazards in extreme rainfall events.
3. To clarify the complexity of the in-situ subsurface hydrogeological condition and increase the model accuracy, the field investigation and well testing are unavoidable tasks.

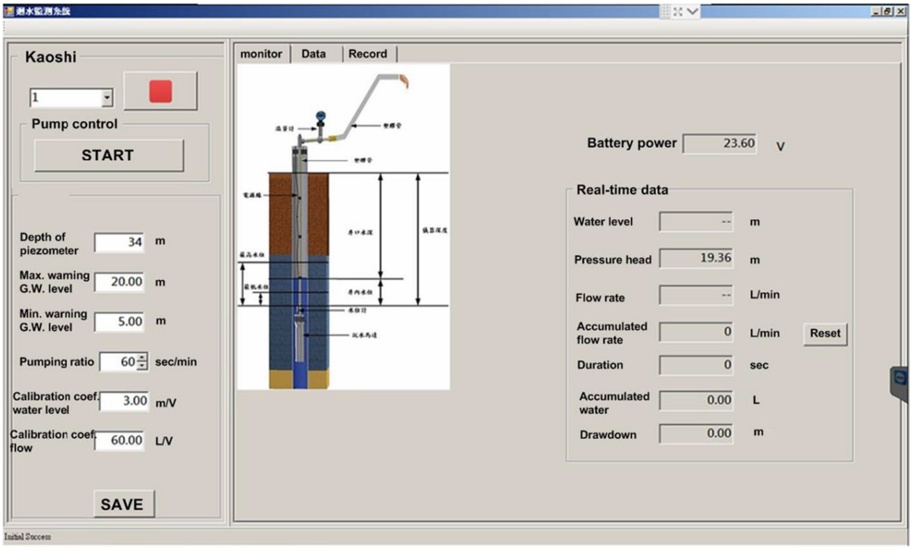

(a) instantaneous data

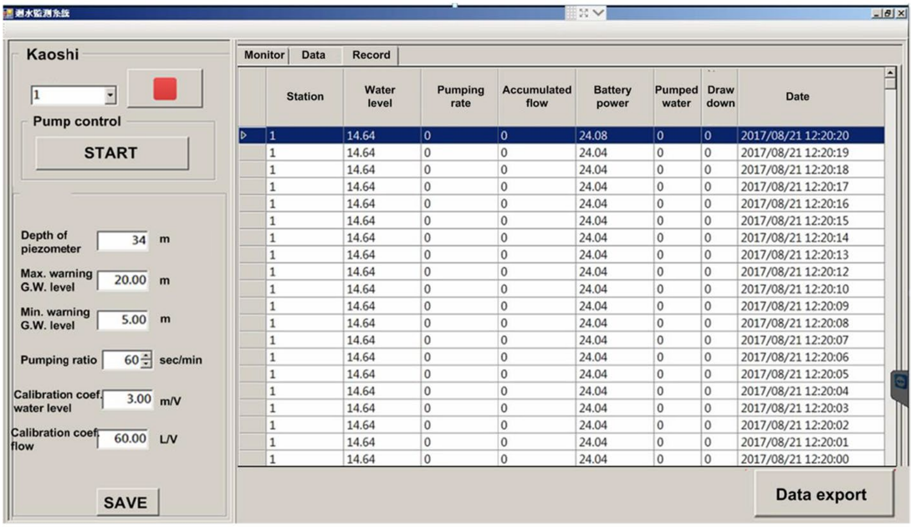

(b) time series data

Fig. 16 Platform for real-time control and monitor

4. The numerical modelling not only identifies the relationship between groundwater exploitation and slope stability but also provides crucial information to design the optimal power capacity and maximize the amount of water that can supply public water used and strengthen the slope stability.

5. When system applied in Kaoshi landslide, each operation can produce at least 450 L and increase 7% in slope stability. The maximum water yield is about 5400 L/day, which is considered a valuable alternative water resource for village residents.

Acknowledgements This work was partially supported by the Ministry of Science and Technology of Taiwan [MOST 107 - 2119 - M - 019 - 001 -]. Additionally, the authors express their gratitude to the Central Geological Survey, Ministry of Economic Affairs (MOEA) of Taiwan for offering hydrogeological raw data used in this study.

References

Chen W, He B, Zhang L, Nover D (2016) Developing an integrated 2D and 3D WebGIS-based platform for effective landslide hazard management. Int J Disaster Risk Reduct 20:26–38. https://doi.org/10.1016/j.ijdrr.2016.10.003

Chou P, Lo H, Hsu S, Lin Y, Huang C (2012) Prediction of hydraulically transmissive fractures using geological and geophysical attributes: a case history from the Mid Jhuoshuei River Basin, Taiwan. Hydrogeol J 20(6):1101–1116. https://doi.org/10.1007/s10040-012-0861-3

Chou P, Hsu S, Chen P, Lin J, Lo H (2014) Fracture-bedrock aquifer studies based on a descriptive statistics of well-logging data: a case study from the Dajia River Basin, Taiwan. Acta Geophys 62(3):564–584. https://doi.org/10.2478/s11600-013-0187-0

Duffield G (2004) AQTESOLV Version 4 user's guide: developer of AQTESOLV. HydroSOLVE, Inc., Reston

El Moulat M, Debauche O, Mahmoudi S, Ait Brahim L, Manneback P, Lebeau F (2018) Monitoring system using internet of things for potential landslides. Procedia Comput Sci 134:26–34. https://doi.org/10.1016/j.procs.2018.07.140

Estrela T, Sancho T (2016) Drought management policies in Spain and the European Union: from traditional emergency actions to drought management plans. Water Policy 118(2):153–176. https://doi.org/10.2166/wp.2016.018

Fang S, Xu L, Zhu Y, Liu Y, Liu Z, Pei H, Zhang H (2013) An integrated information system for snowmelt flood early-warning based on internet of things. Inf Syst Front 17(2):321–335. https://doi.org/10.1007/s10796-013-9466-1

Geetha S, Gouthami S (2017) Internet of things enabled real time water quality monitoring system. Smart Water 2(1):1. https://doi.org/10.1186/s40713-017-0005-y

GEO-SLOPE International Ltd (2007a) Seepage modeling with SEEP/W, user's guide, 2nd edn. GEO-SLOPE International Ltd., Calgary

GEO-SLOPE International Ltd (2007b) Stability modeling with SLOPE/W, user's guide, 2nd edn. GEO-SLOPE International Ltd., Calgary

Hany Abulnour A (2014) Towards efficient disaster management in Egypt. HBRC J 10(2):117–126. https://doi.org/10.1016/j.hbrcj.2013.07.004

Hoang N, Hoa P, Tung L (2014) Study on the accuracy of the numerical modeling of the groundwater movement due to spatial and temporal discretization. VJES 36(4):424–431. https://doi.org/10.15625/0866-7187/36/4/6430

Hong I, Lee J, Cho H (2016) National drought management framework for drought preparedness in Korea (lessons from the 2014–2015 drought). Water Policy 18(s2):89–106. https://doi.org/10.2166/wp.2016.015

Hsu C, Yan H, Hsieh I, Huang H (2012) Investigation of potential landslide disaster on above tribal of Kaoshi Village, Mudan Township. J Slopeland Hazard Prev 11(2):14–23. https://doi.org/10.29995/JSHR.201212.0002

Hutchinson J (1984) Landslides in Britain and their countermeasures. J Jpn Landslide Soc 21(1):1–25. https://doi.org/10.3313/jls1964.21.1

Ku C, Hsu S, Chung M, Chi S, Fei L (2009) An empirical mo.021111111d0e11 for estimating hydraulic conductivity of highly disturbed fractured rocks in Taiwan. Eng Geol 109(3–4):213–223. https://doi.org/10.1016/j.enggeo.2009.08.008

Lai C (2017) Using mountanious groundwater to build up water resources resilient Taiwan. In: Conference on hydrogeology and groundwater resources in mountainous areas, Taipei, Taiwan

Lin D, Hung S, Liu W, Chou J (2018) Evaluation on the efficiency of stability remediation for T16-Tower Pier Slope (T16-SLOPE) of Taipei Mao-Kong Tramway. J Mar Sci Technol 26(3):352–373. https://doi.org/10.6119/JMST.2018.06_(3).0007

Lo H, Hsu S, Chi S, Ku C (2010) Coupled stability analysis of rainfall-induced landslide: a case study in Taiwan piedmont area. ASCE Geotech Spec Publ 204:1–9. https://doi.org/10.1061/41105(378)1

Lo H, Chen P, Chou P, Hsu S (2014) The combined use of heat-pulse flowmeter logging and packer testing for transmissive fracture recognition. J Appl Geophys 105:248–258. https://doi.org/10.1016/j.jappgeo.2014.03.025

Moench A (1997) Flow to a well of finite diameter in a homogeneous, anisotropic water table aquifer. Water Res 33(6):1397–1407. https://doi.org/10.1029/97WR00651

Narendran S, Pradeep P, Ramesh M (2017) An internet of things (IoT) based sustainable water management. In: IEEE global humanitarian technology conference (GHTC). pp 1–6. 10.1109/GHTC.2017.8239320

Okada T (2016) Integrated water resources management and drought risk management in Japan. Water Policy 118(2):70–88. https://doi.org/10.2166/wp.2016.214

Pal I, Ghosh T, Ghosh C (2017) Institutional framework and administrative systems for effective disaster risk governance—perspectives of 2013 cyclone Phailin in India. Int J Disast Risk Res 21:350–359. https://doi.org/10.1016/j.ijdrr.2017.01.002

Soil and Water Conservation Bureau (2011) Management, maintenance and data analysis for grand Lishan area landslide monitoring system. Council of Agriculture, Nantou County, Taiwan

Soil and Water Conservation Bureau (2014) Technical regulations for soil and water conservation. Council of Agriculture, Nantou County, Taiwan

Turner A, Schuster R (1996) Landslides investigation and mitigation-special report 247. National Academy of Sciences, Washington

UNISDR (United Nations International Strategy for Disaster Reduction) (2015) Sendai framework for disaster risk reduction 2015–2030. A/CONF.224/CRP.1. Geneva: UNISDR. https://www.unisdr.org/files/43291_sendaiframeworkfordrren.pdfAccessed 26 Jan 2016.

Verma P, Kumar A, Rathod N, Jain P, Mallikarjun S, Subramanian R, Amrutur B, Sundaresan R (2015) towards an IoT based water management system for a campus. In: IEEE first international smart cities conference (ISC2)

Wang H, Tuo X, Zhang G, Peng F (2013) Panzhihua airport landslide (Oct. 3rd 2009) and an emerging warning system based on the internet of things. J Mt Sci 10(5):873–884. https://doi.org/10.1007/s11629-013-2368-3

Water Resources Agency (2011) Management, hydrological year book of Taiwan-Part I (rainfall data). Ministry of Economic Affairs, Taichung City

World Bank (2015) Strengthening social protection systems to manage disaster and climate risk in Asia and Pacific. World Bank, Washington

Xu X, Zhang L, Sotiriadis S, Asimakopoulou E, Li M, Bessis N (2018) CLOTHO: A Large-scale internet of things based crowd evacuation planning system for disaster management. IEEE Internet Things J 5(5):3559–3568. https://doi.org/10.1109/jiot.2018.2818885

Xi T, Tian Y, Li X, Gao H, Wang W (2018) Pixel-wise depth based intelligent station for inferring fine-grained PM2.5. Future Gener Comput Syst 92:84–92. https://doi.org/10.1016/j.future.2018.08.051

Yang Z, Shao W, Qiao J, Huang D, Tian H, Lei X, Uchimura T (2017) A multi-source early warning system of MEMS based wireless monitoring for rainfall-induced landslides. Appl Sci 7(12):1234. https://doi.org/10.3390/app7121234